From data to models : reducing uncertainty in benefit risk assessment : application to chronic iron overload in children

Bellanti, F.

CHAPTER 7

Model-based optimisation of deferoxamine chelation therapy

Francesco Bellanti, Giovanni C. Del Vecchio, Maria C. Putti, Carlo Cosmi, Ilaria Fotzi, Suruchi D. Bakshi, Meindert Danhof, and Oscar Della Pasqua

Pharm Res – In press

Summary

Purpose: Our endeavour is to show the advantages of a model-based approach to identify key factors that play a role in transfusion-dependent iron overload. We use deferoxamine as a paradigm compound to assess the role of relevant covariates on the underlying disease progression.

Methods: Data from clinical routine practice on 27 patients affected by β-thalassaemia major were used for the analysis. Serum ferritin was selected as the main endpoint of interest for the assessment of iron overload. Its time course was characterised by means of a hierarchical nonlinear mixed effects model, as implemented in NONMEM (7.2.0).

Results: A turnover model best described serum ferritin changes over time, with the effect of blood transfusions introduced as a change in the ferritin conversion rate, whereas the effect of deferoxamine was described by a proportional change in the degradation rate constant (Kout). The inclusion of IOV (57.4 %) on the conversion rate resulted in a significant drop in the OFV (Δ 443) allowing a better description of the individual profiles.

Conclusions: A model-based approach was successfully used to gather further insight into the dynamics of ferritin in transfusion-dependent iron overload. Given the choice of parameterisation, the model may be used as a tool to support clinical practice, including the evaluation of the dose rationale for existing and novel chelating agents.

Abbreviations

ALT	Alanine Aminotransferase
AST	Aspartate Aminotransferase
Css	Steady state concentration
CMPL	Treatment compliance
DFO	Deferoxamine
FT4	Free T4
IIV	Inter-individual variability
IOV	Inter-occasion variability
M&S	Modelling and simulations
NPDE	Normalised predictive distribution error
NTBI	Non-Transferrin Bound Iron
OFV	Objective function value
PKPD	Pharmacokinetic-pharmacodynamic
PRED	Population prediction
RBC	Red blood cells
TSH	Thyroid-Stimulating Hormone
VPC	visual predictive check

7.1 Introduction

Transfusional iron overload

Beta-thalassaemia major is a hereditary blood disorder and patients affected by this disease require regular red blood cell (RBC) transfusions to survive (1–7). Without the chronic transfusion regimen, patients would die before the third decade of life (2,4,5,7,8). Even though a significant improvement has been achieved in the management of the chronic transfusion regimen in the past decades, therapeutic intervention will eventually lead to a series of complications. Iron overload is the most common and relevant one and it is associated with several co-morbidities such as cardiac dysfunction, liver fibrosis, hypogonadism, hypothyroidism, hypoparathyroidism and diabetes mellitus (6,9,10). Cardiac disease caused by myocardial siderosis is the most relevant complication, causing death in 71% of the patients affected by transfusion-dependent diseases (11).

For complex processes such as iron overload, understanding of the dynamics of the disease and its progression is crucial to adequately evaluate the therapeutic intervention. This complexity is also characterised by the fact that the currently accepted biomarker, i.e., blood ferritin is not specific enough to distinguish the effect of transfusion from the influence of other pathological mechanisms such as inflammatory disorders, and/or liver status, which can equally affect the iron interchange between organs and the circulatory system (2,12–14). Consequently, ferritin levels may not provide a direct link for total body or tissue specific iron accumulation at specific time points. On the other hand, changes in ferritin levels over time are still helpful for the management of the disease and maintaining serum ferritin below a threshold of about 2500 µg/L is a widely accepted therapeutic goal (2,3,5–7). However, important clinical questions are not yet fully understood, e.g. how much time is required in order to observe a stable response or to reach clinically meaningful serum ferritin levels.

Iron chelation therapy with chelating agent deferoxamine

Given that human physiology does not have an innate mechanism that allows removal of the iron excess, treatment with iron chelators is therefore vital to prevent its accumulation and related complications (15–18). In the current investigation we attempt to characterise the (patho)-physiological response to the iron chelating agent deferoxamine as a paradigm compound for the assessment of iron dynamics using a model-based approach. Deferoxamine was the first iron chelator approved for human use and has been available for the treatment of iron overload for more than 35 years (2,6,15–19). It is an exadentate chelator that binds iron in a 1:1 ratio. The drug is rapidly absorbed after intramuscular and subcutaneous administration, but it cannot be absorbed orally. In the treatment of iron overload in patients affected by transfusion-dependent haemoglobinopathies several dosing regimens and dose levels have been proposed and used in the past but in the majority of

cases deferoxamine is given as an 8 to 12 hour nightly subcutaneous infusion (5 to 7 days a week) (2,19–21). The serum protein binding is less than 10% and the drug undergoes the following metabolic reactions: transamination and oxidation; beta-oxidation; decarboxylation and N-hydroxylation. The average recommended daily dose varies between 20 and 60 mg/kg and the drug has an half-life of 5.6 hours in patients (20–22).

Deferoxamine binds free iron by preventing the uptake of NTBI (Non-Transferrin Bound Iron) into organs but is also acts within the cell where enters by endocytosis, stimulates the degradation of ferritin via lysosomes and subsequently binds the released iron. The iron bound to deferoxamine is then excreted in urine and faeces (2,6,21,23).
Regardless of numerous limitations associated with the use of deferoxamine, such as poor compliance due to the parenteral administration, inadequate cardiac iron removal and auditory, ocular and neurological toxicities (6,16,18,19,24), deferoxamine is still the most common used therapy for the treatment of iron overload. This widespread use has remained despite the presence of new oral iron chelators.

Given the complexity of the issues highlighted above, our focus is to gain insight into key factors that play a role in iron overload; with the objective of quantifying the therapeutic effect of deferoxamine and identify potential covariates on model parameters describing the underlying disease progression. Furthermore, we propose how modelling and simulation (M&S) can be applied to support decision making in clinical practice, providing a framework to predict changes in the disease status and resulting ferritin response following treatment with existing and novel chelators.

7.2 Methods

Data

The modelling analysis was performed using retrospective clinical data from three different Italian centres: Azienda Ospedaliera Universitaria Consorziale Policlinico di Bari U.O. Pediatria Federico Vecchio; Azienda Ospedaliera Universitaria Policlinico di Sassari Clinica Pediatrica, ASL 1 D.H. per Talassemia; Azienda Ospedaliera di Padova Clinica di Oncoematologia Pediatrica. The study has been conducted in full conformance with the principles of the Declaration of Helsinki and with the local laws and regulations concerning clinical trials. The protocol and the informed consent documents have been formally approved by the relevant research ethics committee of each clinical site.

27 patients affected by transfusion-dependent diseases, receiving deferoxamine as single drug for iron chelation therapy were considered eligible for the retrospective study. Patients receiving chemotherapy, and/or affected by other diseases that require additional blood

transfusions, and/or affected by unrelated endocrine dysfunctions were considered not eligible for the study. Baseline characteristics of the patient population are provided in Table 1. Serum ferritin was the main endpoint of interest and was measured every two to three months; patients contributed with 40.2 observations on average (sd: 17), with a minimum of 4 samples per year. With the same frequency, data on the following variables were collected during the study: height and body weight of the patients, as well as clinical data on TSH, FT4, AST, ALT, glucose, creatinine and ejection fraction. These were considered as potential covariates and were tested during the study to evaluate their influence on the changes in serum ferritin levels.

Table 1. Baseline characteristics of the patient population

	Units	**Median**	**Range**
Age	Years	14.6	6.8-19.9
Weight	Kg	46	17.5-71
Height	Cm	154	111-173
TSH	mIU/L	2.34	0.58-83.2
FT4	ng/dL	1.05	0.73-1.43
AST	U/L	33	7-159
ALT	U/L	56	9-372
Glucose	mg/dL	91	52-444
Creatinine	mg/dL	0.6	0.2-1.12
Ejection Fraction	%	64	35-77
Ferritin	µg/L	2260	393-8500

PK model deferoxamine

As pharmacokinetic samples are not collected in clinical routine monitoring, the model was built using literature data (25) by fitting a mean pharmacokinetic profile in adults patients affected by transfusion-dependent haemoglobinopathies receiving deferoxamine as an 8 hours subcutaneous infusion. A two compartment pharmacokinetic model with zero-order absorption (8 hours subcutaneous infusion) and first-order elimination processes provided an appropriate description of the average steady state concentration (Css^{AV}) for the population of interest. The fitting of the published data is shown in Figure 1.

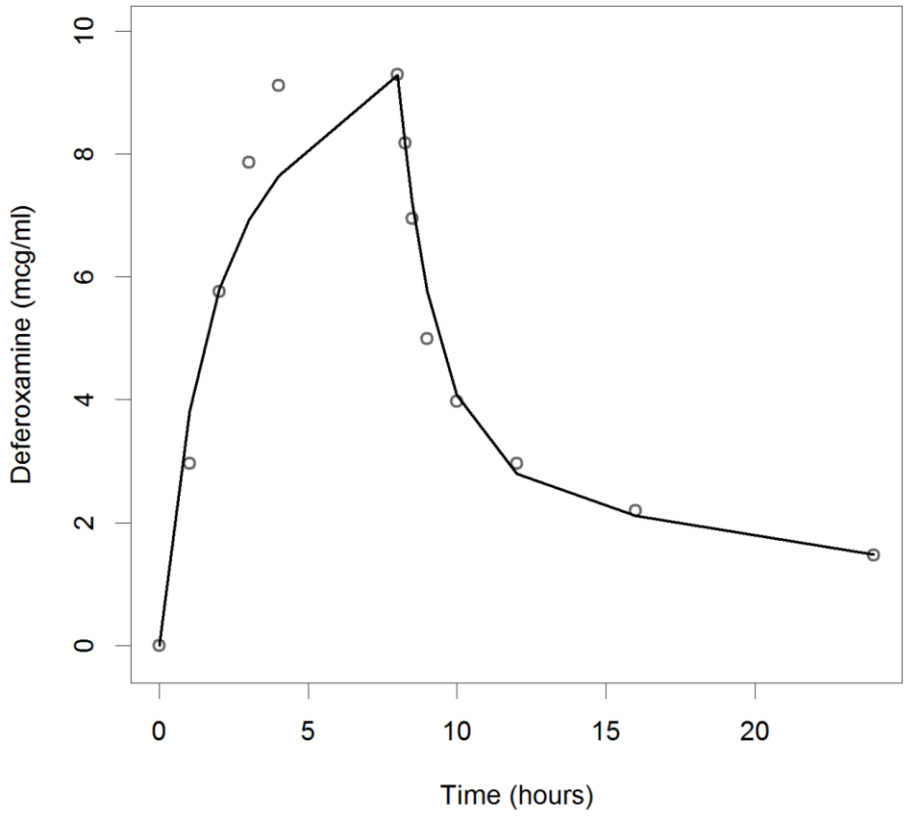

Figure 1. Performance of the pharmacokinetic model of deferoxamine. The circles represent the mean population deferoxamine concentrations reported in literature (23). The solid line represents model prediction.

Assumptions were then made to allow the use of the model to predict exposure in the patient population: 1) the simulations were based on the dosing regimen information collected in the clinical centres and the reported changes to the regimen; and 2) in the absence of quantitative data on adherence to drug therapy, compliance was assumed equivalent to 100%. The role of compliance was assessed in a second phase and details on that are provided in the next paragraphs. Afterwards, fixed allometric scaling (exponent of 0.75 on CL/F and 1.00 on V/F) was used to extrapolate Css^{AV} in adolescents and children. Population prediction (PRED) were used to generate Css^{AV} values in the population of interest.

Disease model iron overload

A disease model for iron overload in patients affected by transfusion-dependent diseases was previously developed by our group [unpublished results]. It consists of an indirect

response model where basal turnover of ferritin levels is depicted by a zero-order production rate (Kin) and a first-order degradation rate (Kout) and the disease component is described by an additive production rate (CRT) triggered by the transfusion regimen which was found to be non-linearly correlated to the disease status (actual ferritin levels).

$$\frac{dFERRITIN}{dt} = Kin + CRT - Kout \times FERRITIN \quad \text{Equation 1}$$

$$CRT = SCL \times e^{-SHP \times FERRITIN} \quad \text{Equation 2}$$

where SCL is a scaling factor and SHP is the shape factor of the correlation. The population parameters of the disease model were kept fixed when performing the PKPD analysis of the retrospective clinical data.

Modelling

The software R (v.2.14.0) was used for statistical summaries as well as data manipulation and preparation for modelling purposes. Nonlinear mixed effects modelling was instead performed in NONMEM version 7.2 (Icon Development Solutions, USA).

Model building criteria included: (i) successful minimisation, (ii) standard error of estimates, (iii) number of significant digits, (iv) termination of the covariance step, (v) correlation between model parameters and (vi) acceptable gradients at the last iteration. Comparison of hierarchical models was based on the likelihood ratio test. Goodness of fit was assessed by graphical methods, including population and individual predicted vs. observed concentrations, conditional weighted residual vs. observed concentrations and time, correlation matrix for fixed vs. random effects, correlation matrix between parameters and covariates and normalised predictive distribution error (NPDE) (26).

Fixed and random effects were introduced into the model in a stepwise manner. Inter-individual variability in the parameters was assumed to be log-normally distributed. A parameter value of an individual *i* (post hoc value) is therefore given by the following equation:

$$\theta_i = \theta TV * e^{\eta i}$$

in which θTV is the typical value of the parameter in the population and ηi is assumed to be random variable with zero mean and variance ω^2. Residual variability, which comprises measurement and model error, was described with a proportional error model. This means for the jth observed concentration of the ith individual, the relation Y_{ij}:

$$Y_{ij} = F_{ij} + \varepsilon_{ij} * W$$

where F_{ij} is the predicted concentration and ε_{ij} the random variable with mean zero and variance σ^2. W is a proportional weighing factor for ε.

Different concentration-effect relationships (e.g., Emax model, linear model, etc.) were tested on the disease model presented in equation 1 to quantify the effect of deferoxamine on serum ferritin levels. Css^{AV} levels, generated with the PK model described above were used in the drug model as a measure of deferoxamine exposure. The effect of deferoxamine (DFO) was introduced as proportional change in the degradation rate (Kout) of ferritin as shown in equation 3 which is derived from equation 1.

$$\frac{dFERRITIN}{dt} = Kin + CRT - Kout \times FERRITIN \times (1 + DFO) \quad \text{Equation 3}$$

$$DFO = SLP \times SCss^{AV} \quad \text{Equation 4}$$

where DFO is the effect of deferoxamine on the Kout of the disease model, SLP is the slope parameter of the concentration-effect relationship, and $SCss^{AV}$ is the steady state concentrations simulated with the deferoxamine PK model.
In addition, the disease model parameters, the scaling (SCL) and the shape (SHP) factors presented in equation 2 were found to be non-linearly correlated to the actual disease status according to the following relationships:

$$SCL_i = SCL_{ref} \times \left(\frac{FERRITIN}{FERRITIN_{med}}\right)^{\theta x} \quad \text{Equation 5}$$

$$SHP_i = SHP_{ref} \times \left(\frac{FERRITIN}{FERRITIN_{med}}\right)^{\theta x} \quad \text{Equation 6}$$

where SCL_{ref} and SHP_{ref} are the reference parameters in the population of interest, SCL_i and SHP_i are the individual parameters, $FERRITIN_{med}$ is the median ferritin value in the population of interest and θx is the estimated exponent of the relationship.
The evaluation of the final model was based on graphical and statistical methods, including visual predictive checks (27). Bootstrap was used to identify bias, stability and accuracy of the parameter estimates (standard errors and confidence intervals). The bootstrap procedures were performed in PsN v3.5.3 (University of Uppsala, Sweden) (28), which automatically generates a series of new data sets by sampling individuals with replacement from the original data pool, fitting the model to each new data set.

Assessing the role of compliance

At the initial stage of the model-building phase, the model was not able to appropriately describe the data (Figure 2), under the assumption that the patients represent a single population. However, two different profiles were observed in the data, which prompted us consider dichotomising the data into responders and non-responders. An arbitrary definition was used based on the observed ferritin levels: the responders showed very stable profiles around 2500 µg/L serum ferritin, whereas the non-responders showed very steep increases in ferritin levels and appeared not to be able to return to a less severe state of the disease. A mixture model improved the quality of the fitting, but did not allow an adequate characterisation of the individual profiles.

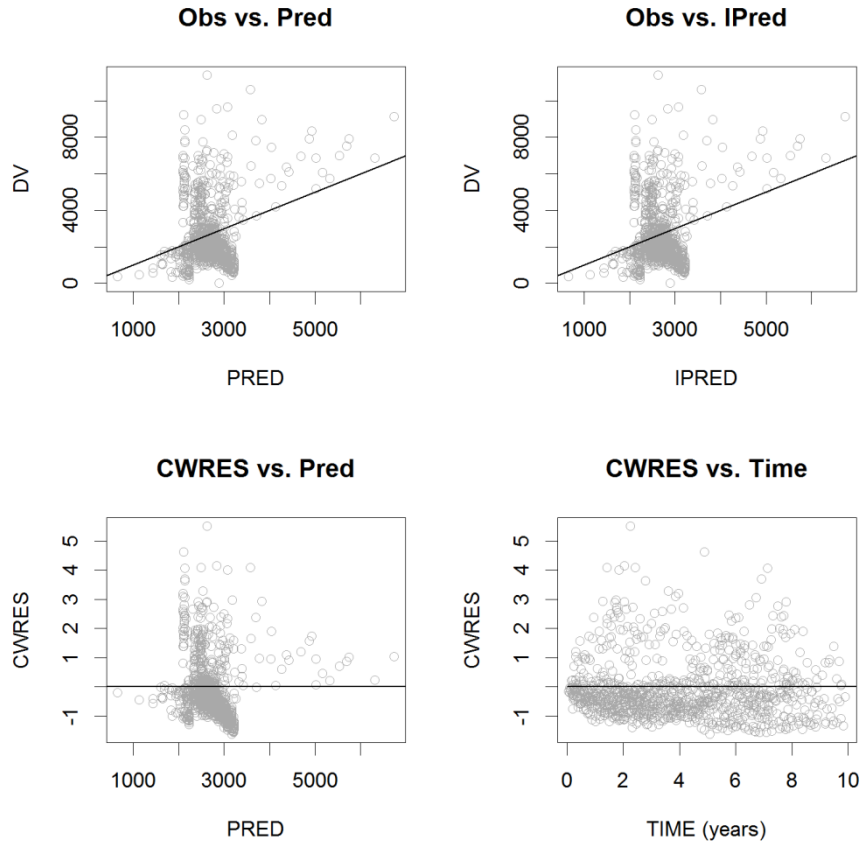

Figure 2. Goodness-of-fit plots of the model without the inclusion of compliance. Upper panels show the observed data (Obs) vs. population predictions (Pred) (left) and the observed data vs. individual predictions (IPred) (right). Lower panels show the conditional weighted residuals (CWRES) vs. population predictions (left) and the CWRES vs time (left).

We have therefore investigated other potential mechanisms and explanatory factors associated with the different response profiles based on the information available in the

literature. Treatment compliance was found to be the major cause of differences in ferritin levels. In the papers by Gabutti et al. (29) and Galanello et al. (30) serum ferritin profiles are quite stable over the observational period (Figures 3 and 1 respectively) as in our responder group and compliance is in both cases higher than 95%. In other investigations (20,29,31) Kaplan-Meier analyses show the relationship between survival and treatment compliance, providing evidence of the fact that poor adherence has a crucial impact on the clinical outcome. In particular the work by Olivieri et al. (31) shows how survival can directly be linked to the observed ferritin levels.

The absence of quantitative data on treatment compliance in our retrospective study did not allow us to directly select this variable to account for such differences, which represented a clear obstacle for the analysis. To overcome this issue we used the work carried out by Olivieri et al. (31) as a reference and we derived a new variable (CMPL) based on the percentage of observations for each patient above the threshold of 2500 µg/L ferritin. The new variable (CMPL) was introduced in the model as follows:

$$DFO = SLP \times {TC_{ss}}^{AV} \qquad \text{Equation 7}$$

$${TC_{ss}}^{AV} = {SC_{ss}}^{AV} \times (1 - CMPL) \qquad \text{Equation 8}$$

where DFO is the effect of deferoxamine, SLP is the slope parameter of the concentration-effect relationship, and $TCss^{AV}$ are the "true" steady state concentrations after accounting for the impact of treatment compliance (CMPL). $TCss^{AV}$ are derived from the simulated steady state concentrations ($SCss^{AV}$) corrected by treatment compliance as shown in equation 7.

The implementation of treatment compliance provided a significant increase in the fitting performances of the model (as shown in Figures 3 and 4) and allowed a more accurate quantification of the therapeutic intervention.

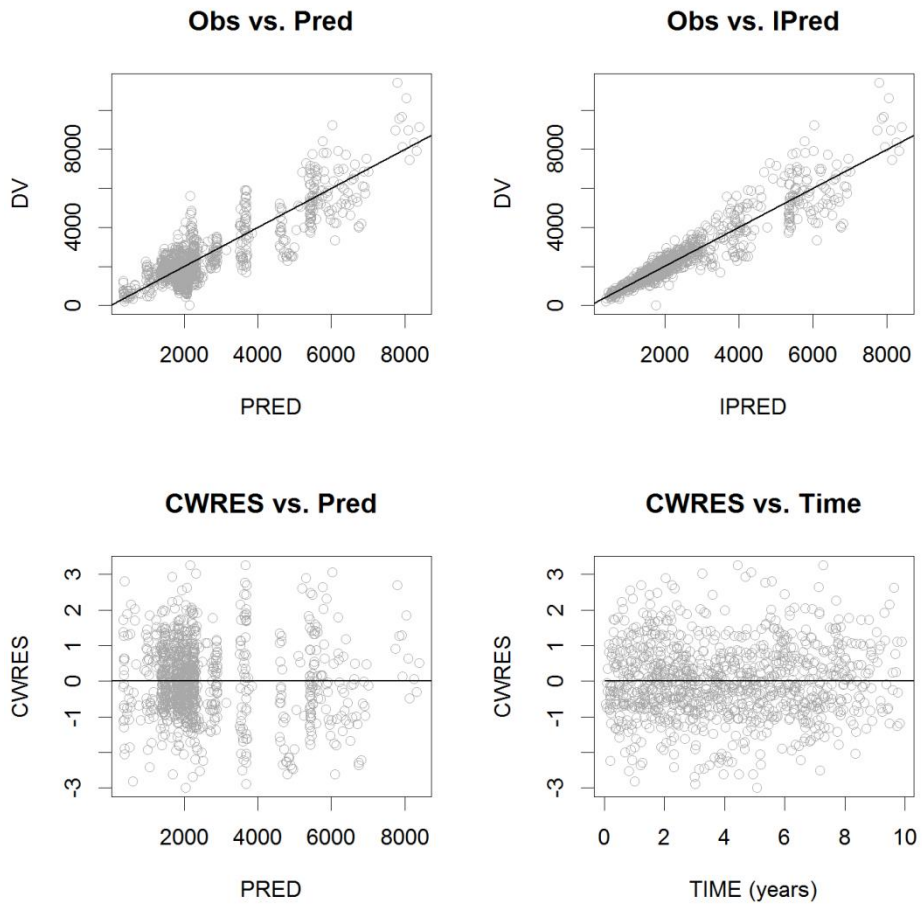

Figure 3. Goodness-of-fit plots of the final model. Upper panels show the observed data (Obs) vs. population predictions (Pred) (left) and the observed data vs. individual predictions (IPred) (right). Lower panels show the conditional weighted residuals (CWRES) vs. population predictions (left) and the CWRES vs time (left).

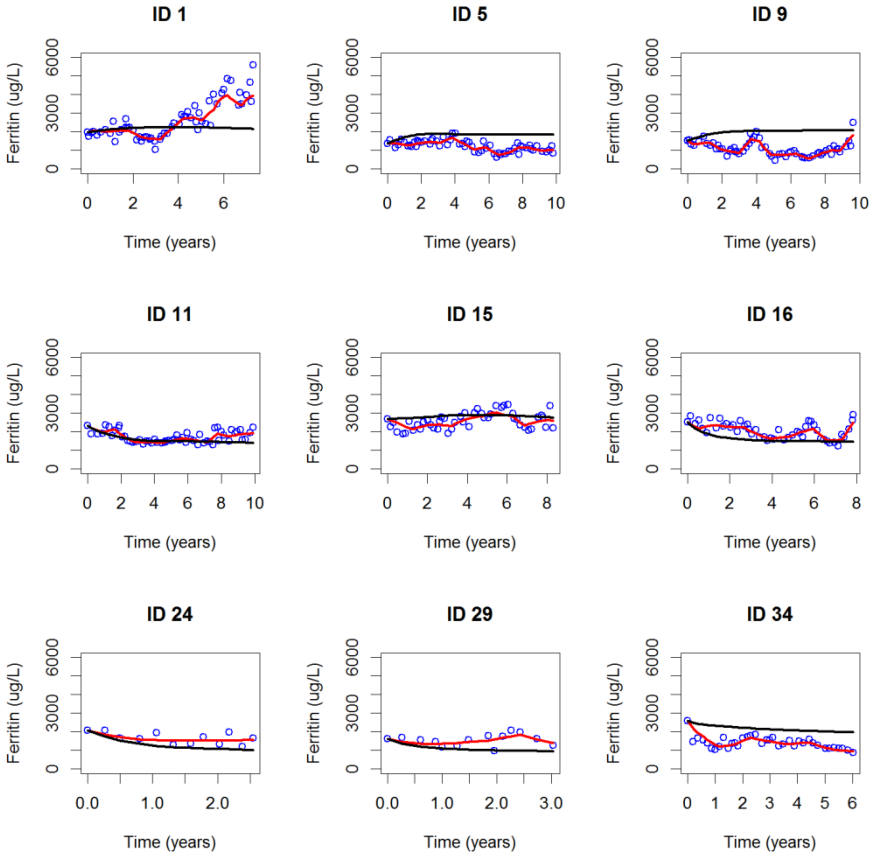

Figure 4. Individual plots of 9 randomly selected patients: observed data are plotted using blue circles; the black solid line represents the population prediction (Pred) and the red solid line represents the individual predictions (IPred).

Model Simulations

Simulations were performed to investigate the impact of different exposure levels and various compliance scenarios on the clinical evaluation of serum ferritin levels. Time to reach 2500 µg/L serum ferritin (threshold between moderate and severe iron overload (2,6,20,31,32)) was chosen as a comparison measure between different scenarios. The differential equation solver ode15s from the software MATLAB (version R2010b) was used for the purpose of model simulations, whereas the software R (v.2.14.0) was used for graphical summaries. The ode15s which is a multistep solver and uses numerical differentiation formulas is particularly suitable for stiff systems (33,34).

Three dosing regimens (30, 45 and 60 mg/kg/day for 5 days a week) were used to generate Css^{AV} in a patient population with body weight ranging from 15 to 75 kg. This allowed evaluating the impact of different exposures on the endpoint of interest (time to reach the threshold). Each exposure level was then tested on patients starting at different baselines

ranging from 3000 to 12000 μg/L serum ferritin. In this set of simulations the exposure was assumed to be constant over time.

In addition, simulations were used to evaluate the impact of various compliance scenarios on changes in ferritin levels. Our main interest in this case was to show how the model can be used prospectively in the clinical practice to evaluate a priori any given situation. To present and discuss the results of these simulations, given the large number of scenarios evaluated, we considered only a virtual patient of 45 kg receiving 45 mg/kg/day deferoxamine 5 days per week (representative of the mean patient in the population under investigation). The different scenarios investigated are presented in Table 2; compliance is stratified per 1 year, 6, 2 and 1 months.

Table 2. Simulation scenarios for the evaluation of different compliance levels

		Number of missed doses in the stratification period				
		Single doses (Random)	**Consecutive doses (Drug holidays)**			
		Stratification				
	% of missed doses	**1 year**	**1 year**	**6 months**	**2 months**	**1 month**
Scenario 1	10%	25	25	/	5	/
Scenario 2	20%	50	50	25	10	5
Scenario 3	30%	75	75	/	15	/
Scenario 4	40%	100	100	50	20	10
Scenario 5	50%	125	125	/	25	/
Scenario 6	60%	150	150	75	30	15
Scenario 7	70%	175	175	/	35	/
Scenario 8	80%	200	200	100	40	20
Scenario 9	90%	225	225	/	45	/

Full adherence is equivalent to 250 doses per year

The iterations were stopped if more than 5 years were needed to reach the threshold of 2500 μg/L serum ferritin. As proposed in the work carried out by Piana et al. (35), the five scenarios selected try to cover different compliance patterns that may occur in the presence of a chronic regimen. Scenario 1 with single doses missed at random reflects poor quality of execution, whereas the other scenarios provide a range of options that reflect different patterns and durations of drug holidays.

7.3 Results

Disease model

The use of a disease model describing the impact of blood transfusions on serum ferritin was expanded to include the effects of chelation therapy. The effect of blood transfusions was introduced as a conversion rate on the production rate of ferritin and was found in the previous analysis to be inversely correlated to the disease status as shown in equation 1 and 2. In addition, the disease model parameters, the scaling (SCL) and the shape (SHP) factors presented in equation 2 were found to be non-linearly correlated to the actual disease status. Their inclusion in the model provided a significant decrease in the objective function value (OFV) and allowed a better description of the data. Furthermore, the inclusion of inter-occasion variability (IOV = 57.4 %) on the conversion rate resulted in a significant drop in the OFV (Δ 443) allowing a better description of the individual profiles.

Drug model

The effect of deferoxamine (DFO) was introduced in a proportional way on the degradation rate (Kout) of ferritin. Furthermore, the implementation of treatment compliance as a factor on the exposure of deferoxamine improved considerably the data fitting and the model performance, as well as the inclusion of inter-individual variability (IIV) on the slope parameter, which reduced significantly the OFV and improved goodness of fit and visual predictive check (VPC) diagnostics. An overview of the final model parameters and bootstrap results is presented in Table 3.

Table 3. Parameter estimates of the PKPD model of deferoxamine

Parameter	Estimate	Bootstrap (mean)	CV (%)
Kin (mcg/h)	0.0002 (FIX)	/	/
Kout (h-1)	0.0000045 (FIX)	/	/
SHP (h-1)	0.00026 (FIX)	/	/
SCL (mcg/h)	0.383 (FIX)	/	/
Slope (mcg/conc)	4.81	5.16	15.7
Error Proportional	-0.173	-0.17	6.5
DIS exp on SHP	1.29	1.08	57.4
DIS exp on SCL	0.845	0.67	51.9
IIV on Slope	0.082	0.105	80.9
IOV on CRT	0.252	0.29	43.1

Internal model validation diagnostics were satisfactory. Individual predicted profiles and goodness-of-fit plots as shown in Figures 3 and 4, as well as VPC (Figure 5) reveal that the

model provides an adequate and non-biased description of the data. In addition, NPDE summaries (Figure 6) show that the discrepancy between predicted and observed values can be assumed to be normally distributed.

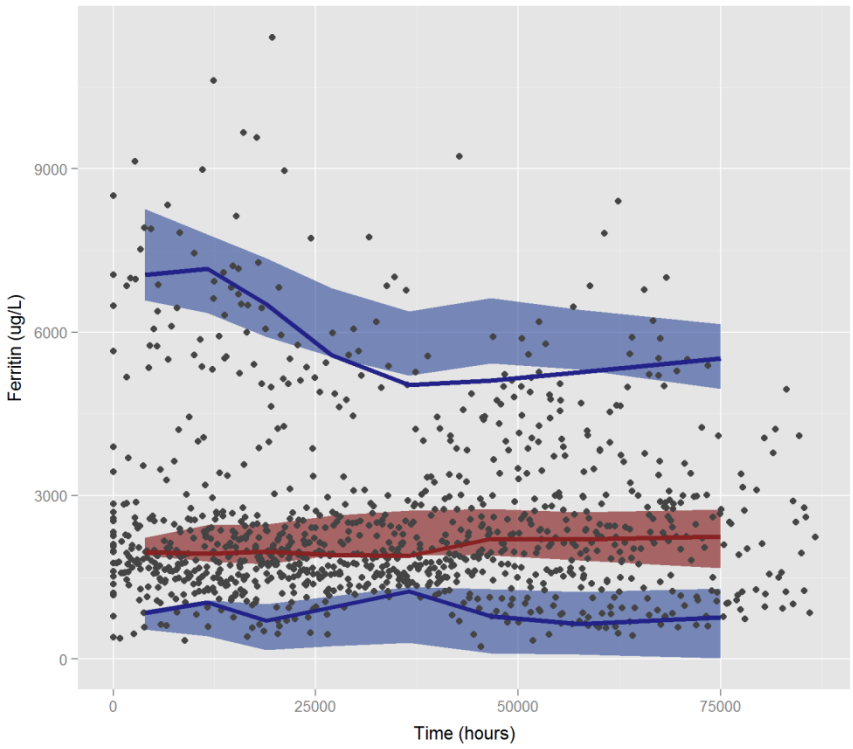

Figure 5. Visual predictive check: observed data are plotted using grey circles; the red solid line represents the median of the observed data; the blue solid lines represent the 5th and 95th percentiles of the observed data. The red shaded area represents the 95th CI of the median of the simulated data; the blue shaded areas represent the 95th CI of the 5th and 95th percentiles of the simulated data.

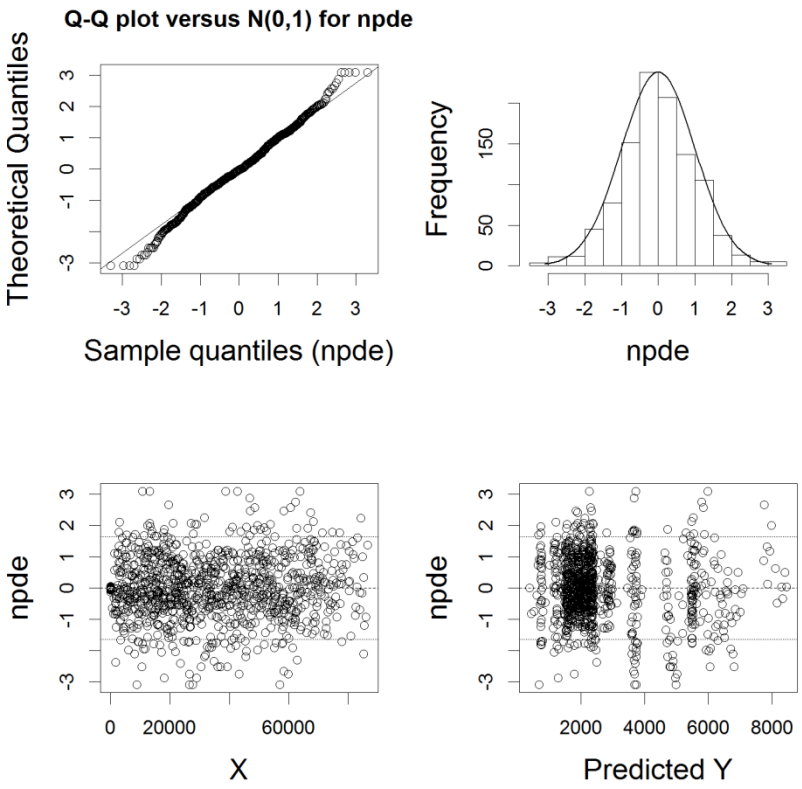

Figure 6. NPDE: normalised prediction distribution errors. Upper panels show the QQ-plot of the distribution of the NPDEs for a theoretical N (0, 1) distribution (left) and the histogram of the distribution of the NPDE together with the density of the standard normal distribution (right). Lower panels show the NPDEs vs. time (left) and NPDEs vs. individual predictions (right).

Model Simulations

The impact of different exposure levels and various compliance scenarios on the clinical evaluation of serum ferritin levels was evaluated through model simulations. The results of the effect of different exposure levels in virtual patients characterised by different body weights and starting at different ferritin baseline levels are presented in Figure 7 for the following dosing regimen respectively: 30, 45 and 60 mg/kg/day for 5 days a week. Results clearly show that in the absence of an adequate exposure to the chelating agent an appropriate clinical response cannot be achieved. The model provides also the opportunity to evaluate a priori the most suitable dosing regimen to achieve a desired therapeutic goal.

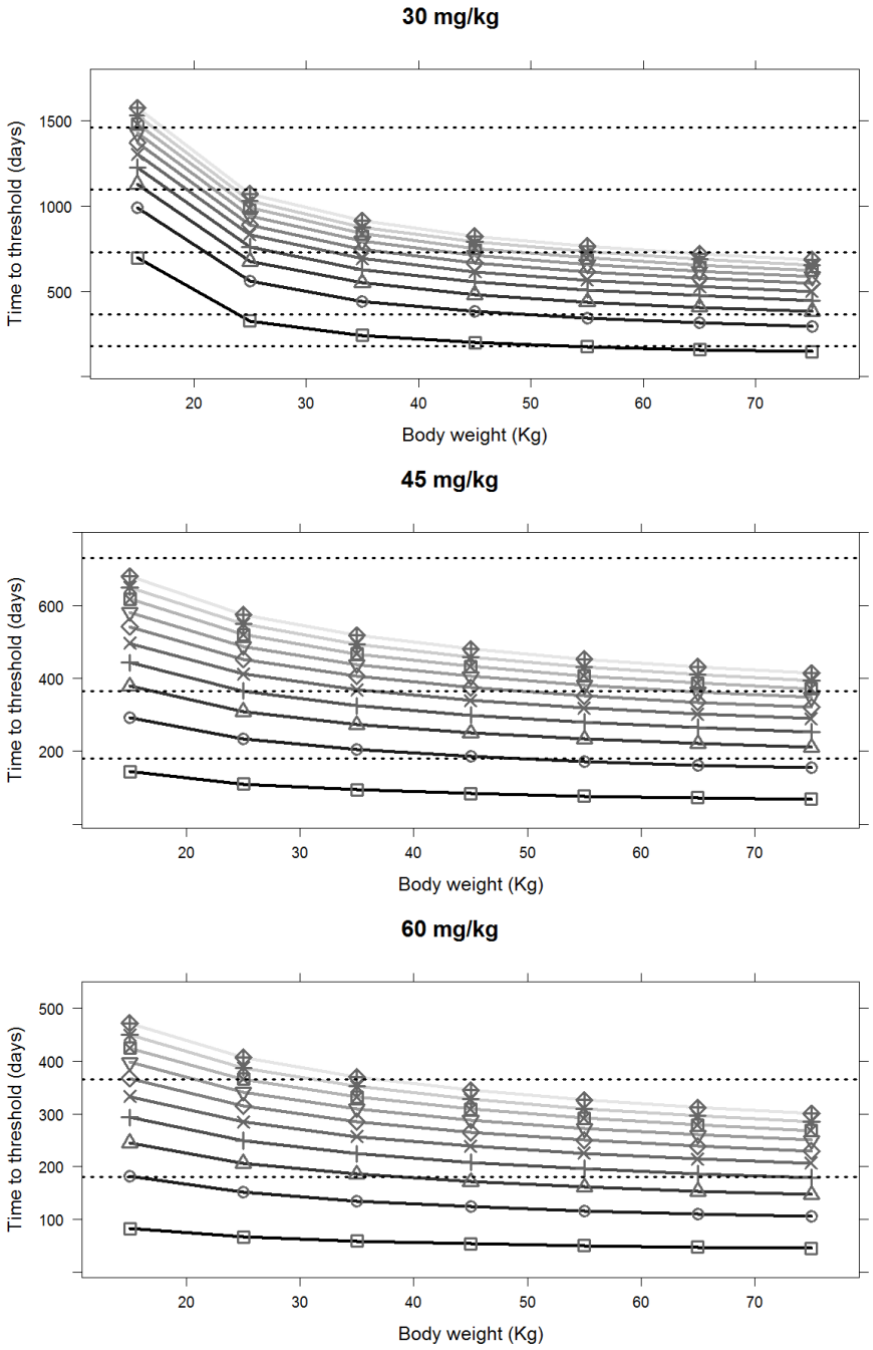

Figure 7. Time to reach a threshold of 2500 ug/L of serum ferritin based on different exposure levels in patients with different body weights (15 to 75 kg). The different panels show three scenarios where 30, 40 and 45 mg/kg dosing regimen have been evaluated. Each line represents a different starting baseline ferritin level (darker to lighter shows an increase in the starting baseline levels): square, circle, triangle with point up, plus, cross, diamond, triangle with point down, square cross, star and diamond plus represent respectively 3000, 4000, 5000, 6000, 7000, 8000, 9000, 10000, 11000 and 12000 ug/L of the starting baseline ferritin.

We have also investigated in one virtual patient of 45 kg receiving 45 mg/kg/day deferoxamine 5 days per week the impact of different compliance patterns in achieving a specific response, which was defined as time to reach the threshold of 2500 µg/L serum ferritin. Several conclusions can be derived from the results of the simulations: 1) if single doses are missed at random (reflecting poor quality of execution) (Figure 8 – scenario 1) as compared to doses missed consecutively (drug holidays) (Figure 8 – scenario 2) over a period of 1 year, a better and faster response is achieved; 2) if doses are missed consecutively over a given period of time, the shorter the period the better the clinical response as shown in Figure 8 – scenarios 2 to 5) in all the scenarios, if more than 60 % of the doses are missed (treatment compliance is lower than 40%) the therapeutic intervention is not effective; finally 4) a reduction in treatment compliance, especially when moving from 30 to 60% of missed doses clearly shows a significantly slower response indicating that even though the desired therapeutic outcome will be achieved the time to reach this goal might not be sustainable by the patient.

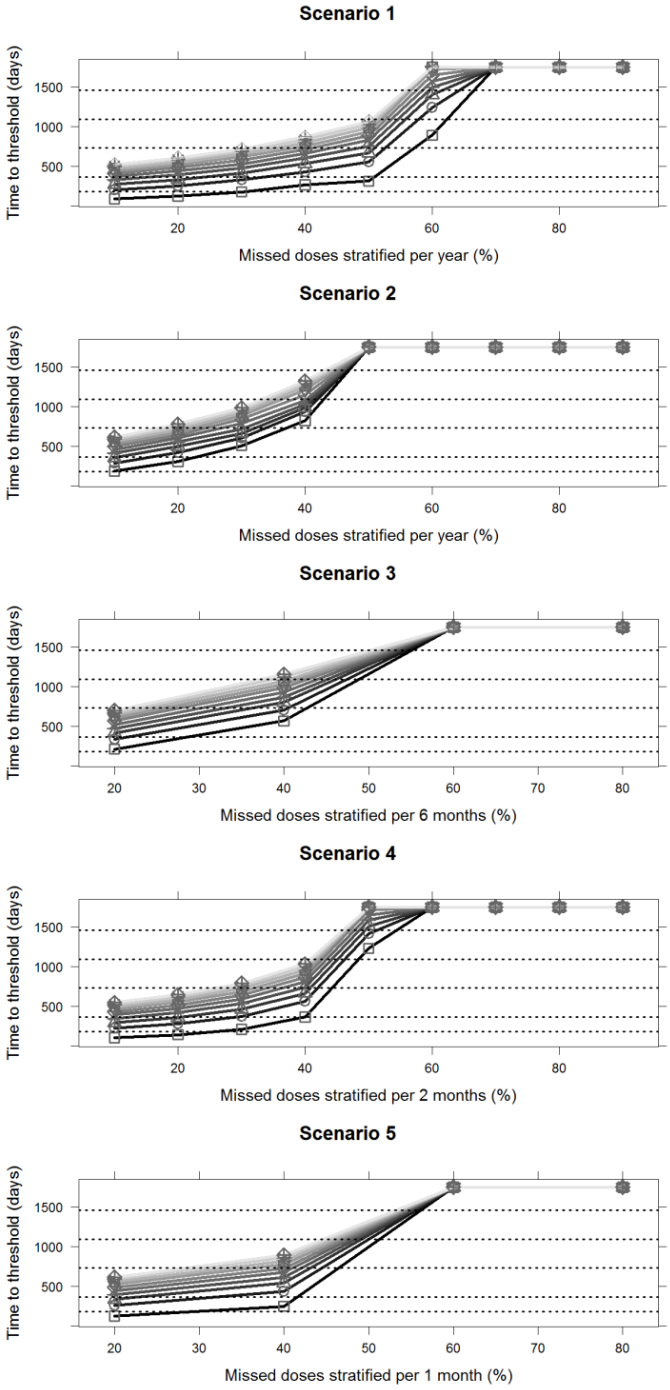

Figure 8. Time to reach a threshold of 2500 mcg/L of serum ferritin based on different compliance scenarios (10 to 90 % of missed doses). The different panels show five scenarios where different compliance patterns have been evaluated (see table II). Each line represents a different starting baseline ferritin level (darker to lighter shows an increase in the starting baseline levels): square, circle, triangle with point up, plus, cross, diamond, triangle with point down, square cross, star and diamond plus represent respectively 3000, 4000, 5000, 6000, 7000, 8000, 9000, 10000, 11000 and 12000 ug/L of the starting baseline ferritin.

7.4 Discussion

A model-based approach was proposed here to understand the implications of iron chelation therapy with deferoxamine on ferritin levels in patients affected by transfusion-dependent diseases. The complexity of the system requires an integrated approach that allows exploring the dynamics of the disease and its progression. A drug model was incorporated successfully into a disease model previously developed aimed at the characterisation of ferritin levels in this population. The model was evaluated using statistical and graphical criteria of goodness-of-fit and predictive performance measures as shown in table III and figures 3 to 6. The analysis reveals a strong effect of the disease status on the overall iron/ferritin conversion rate, and highlights also the role of treatment (drug exposure and compliance patterns) on the overall response and disease progression. In addition, the inclusion of IOV (57.4 %) allowed achieving a better description of individual profiles. Such a value of IOV appears to be influenced by larger intra-individual variability at higher serum ferritin levels where other mechanisms such as inflammatory disorders, and/or liver status play a role in determining the absolute ferritin value. Unfortunately, the lack of information on these variables allowed us only to take a stochastic approach for the quantification of such differences.

Parameterisation of iron chelation

Deferoxamine binds iron at different extracellular levels, and within the cell it targets lysosomal ferritin iron by stimulating ferritin degradation (23). Given that with the available data we could not distinguish among the different actions of deferoxamine, we decided to parameterise the drug effect as a proportional factor influencing the Kout of the turnover model. Furthermore, the same parameterisation would allow exploring the effect of other chelating agents: for example, oral chelators such as deferiprone and deferasirox also act intracellularly as deferoxamine, though targeting a different pathway (i.e., cytosolic ferritin iron) (23).

Clinical application

Model simulations were used to investigate the impact of different exposure levels and various compliance scenarios on serum ferritin levels. Results show that inadequate iron chelation therapy with sub-therapeutic exposure (Figure 7) as well as poor adherence to the assigned dosing regimen (Figure 8) would significantly increase the time required to achieve a desired clinical response, and in some cases (e.g., with treatment compliance lower than 40%) patients would not achieve at all the therapeutic goal. Even though these results might seem rather obvious, we are aware that clinically relevant changes in serum ferritin levels are observed over a long period of time and often crucial decisions have to be made before the clinical evidence is available. This availability of this model shows an opportunity to

explore different scenarios that have been so far evaluated empirically in clinical practice. For example, model simulations allow evaluating whether a compromise between lower exposure, aimed at a possible reduction in acute side effects is compensated by acceptable increase in the time to achieve the therapeutic goal. Likewise, it may be possible to evaluate the importance of different compliance patterns for the available chelating agents, yielding a more quantitative estimate of the changes in ferritin levels and /or risk of clinical failure. This information can then be used to support the decision making and to optimise the therapeutic intervention.

Limitations

Some limitations must be discussed in the context of this analysis. First of all, we used a PK model developed on literature data, which allowed us using mean population data and derive individual information based only on fixed allometric scaling. A more structured analysis of the PK of deferoxamine would reduce the uncertainty around the simulated exposure and would allow us explaining the variability in PK that propagates into the pharmacodynamics. On the other hand, we believe that the approach taken allowed us to characterise differences in the pharmacokinetics that we would have not been able to define only with information on the dosing regimen; e.g., changes in size are accounted for based on allometric scaling.

A second aspect is the role of compliance in the context of this analysis. The absence of quantitative data on treatment adherence in the population under investigation was a clear impediment. To overcome this issue we used the observed data to generate a variable that would allow us to have a gradient of treatment compliance. This decision was supported by the information available in the literature; we found clear evidence that high compliance leads to stable ferritin levels over time and that poor adherence to deferoxamine therapy is strongly correlated to a poor clinical outcome as nicely depicted in the work by Gabutti et al. (29) (Kaplan-Meier analysis presented in Figure 6). This was confirmed by a few other publications (20,30,31,36) and gave us the confidence that the approach taken would be robust enough to meet the purposes of this analysis.

Conclusion

In conclusion, we were able to gather further insights in the dynamics of a rather complex process such as iron overload using a model-based approach. Bearing in mind the limitations discussed and the relative level of uncertainty, the model has proven to be a useful tool to support decision making in clinical practice in the context of transfusion-dependent haemoglobinopathies. In addition, this approach will enable further evaluation of the dose rationale for existing and novel chelating agents.

References

1. Gibbons R, Higgs DR, Old JM, Olivieri NF, Swee Lay T, Wood WG. The Thalassaemia Syndromes - Fourth Edition. Blackwell Sci. 2001;

2. Galanello R, Origa R. Beta-thalassemia. Orphanet J Rare Dis. 2010 Jan;5:11.

3. Ginzburg Y, Rivella S. B-Thalassemia: a Model for Elucidating the Dynamic Regulation of Ineffective Erythropoiesis and Iron Metabolism. Blood. 2011 Oct 20;118(16):4321–30.

4. Rebulla P. Blood transfusion in beta thalassaemia major. Transfus Med. 1995 Dec;5(4):247–58.

5. Rebulla P, Modell B. Transfusion requirements and effects in patients with thalassaemia major. Lancet. 1991;337:277–80.

6. Rund D, Rachmilewitz E. Beta-Thalassemia. N Engl J Med. 2005;353:1135–46.

7. Thalassaemia International Federation (TIF). Guidelines for the clinical management of thalassaemia. 2008.

8. Porter J, Huehns E. Transfusion and exchange transfusion in sckle cell anaemias, with particular reference to iron metabolism. Acta Haematol. 1987;78:198–205.

9. Cunningham MJ, Macklin E a, Neufeld EJ, Cohen AR. Complications of beta-thalassemia major in North America. Blood. 2004 Jul 1;104(1):34–9.

10. Borgna-Pignatti C, Rugolotto S, De Stefano P, Zhao H, Cappellini MD, Del Vecchio G, et al. Survival and complications in patients with thalassemia major treated with transfusion and deferoxamine. Haematologica. 2004;89(10):1187–93.

11. Borgna-Pignatti C, Cappellini MD, De Stefano P, Del Vecchio GC, Forni GL, Gamberini MR, et al. Survival and complications in thalassemia. Ann N Y Acad Sci. 2005 Jan;1054:40–7.

12. Brittenham GM, Cohen a R, McLaren CE, Martin MB, Griffith PM, Nienhuis a W, et al. Hepatic iron stores and plasma ferritin concentration in patients with sickle cell anemia and thalassemia major. Am J Hematol. 1993 Jan;42(1):81–5.

13. Lipschitz D, Cook J, Finch C. A clinical evaluation of serum ferritin as an inndex of iron stores. N Engl J Med. 1974;290(22):1213–6.

14. Puliyel M, Sposto R, Berdoukas V a, Hofstra TC, Nord A, Carson S, et al. Ferritin trends do not predict changes in total body iron in patients with transfusional iron overload. Am J Hematol. 2014 Apr;89(4):391–4.

15. Cappellini MD, Pattoneri P. Oral iron chelators. Annu Rev Med. 2009 Jan;60:25–38.

16. Kwiatkowski JL. Oral iron chelators. Pediatr Clin North Am. 2008 Apr;55(2):461–82.

17. Musallam KM, Taher AT. Iron chelation therapy for transfusional iron overload: a swift evolution. Hemoglobin. 2011 Jan;35(5-6):565–73.

18. Shander A, Sweeney J. Overview of Current Treatment Regimens in Iron Chelation Therapy. US Hematol. 2009;2(1):56–9.

19. Fisher S, Brunskill S, Doree C, Gooding S, Chowdhury O, Roberts D. Desferrioxamine mesylate for managing transfusional iron overload in people with transfusion-dependent thalassaemia (Review). cochrane Libr. 2013;(8).

20. Brittenham G, Griffith P, Nienhuis A, McLaren C, Young N, Tucker E, et al. Efficacy of deferoxamine in preventing complications of iron overload in patients with thalassemia major. N Engl J Med. 1994;331(9):567–73.

21. Novartis Pharmaceuticals UK. Deferoxamine summary of product characteristics.

22. Porter J. Deferoxamine pharmacokinetics. Semin Hematol. 2001 Jan;38(1 Suppl 1):63–8.

23. Theil EC. Mining ferritin iron: 2 pathways. Blood. 2009 Nov 12;114(20):4325–6.

24. Bentur Y, Koren G, Tesoro A, Carley H, Olivieri N, Freedman MH. Comparison of deferoxamine pharmacokinetics between asymptomatic thalassemic children and those exhibiting severe neurotoxicity. Clin Pharmacol Ther. 1990 Apr;47(4):478–82.

25. Porter JB, Rafique R, Srichairatanakool S, Davis B a, Shah FT, Hair T, et al. Recent insights into interactions of deferoxamine with cellular and plasma iron pools: Implications for clinical use. Ann NY Acad Sci. 2005 Jan;1054:155–68.

26. Comets E, Brendel K, Mentré F. Computing normalised prediction distribution errors to evaluate nonlinear mixed-effect models: the npde add-on package for R. Comput Methods Programs Biomed. 2008 May;90(2):154–66.

27. Hooker AC, Staatz CE, Karlsson MO. Conditional weighted residuals (CWRES): a model diagnostic for the FOCE method. Pharm Res. 2007 Dec;24(12):2187–97.

28. Lindbom L, Ribbing J, Jonsson EN. Perl-speaks-NONMEM (PsN)--a Perl module for NONMEM related programming. Comput Methods Programs Biomed. 2004 Aug;75(2):85–94.

29. Gabutti V, Piga A. Results of Long-Term Iron-Chelating Therapy. Acta Haematol. 1996;95:26–36.

30. Galanello R, Kattamis A, Piga A, Fischer R, Leoni G, Ladis V, et al. A prospective randomized controlled trial on the safety and efficacy of alternating deferoxamine and deferiprone in the treatment of iron overload in patients with thalassemia. Haematologica. 2006;91:1241–3.

31. Olivieri N, Nathan D, MacMillan J, Wayne A, Liu P, McGee A, et al. Survival in Medically Treated Patients with Homozygous β-Thalassemia. N Engl J Med. 1994;331:574–8.

32. Modell B, Khan M, Darlison M. Survival in β-thalassaemia major in the UK: data from the UK Thalassaemia Register. Lancet. 2000;355(9220):2051–2.

33. Shampine L, Reichelt M. The MATLAB ODE Suite. SIAM J Sci Comput. 1997;18:1–22.

34. Shampine L, Reichelt M, Kierzenka J. Solving Index-1 DAEs in MATLAB and Simulink. SIAM Rev. 1999;41:538–52.

35. Piana C. Adherence to antiretroviral combination therapy in children. 2013. p. 181–92.

36. Kattamis A, Dinopoulos A, Ladis V, Berdousi H, Kattamis C. Variations of ferritin levels over a period of 15 years as a compliance chelation index in thalassemic patients. Am J Hematol. 2001 Dec;68(4):221–4.